arXiv:cond-mat/0407131v1 [cond-mat.str-el] 6 Jul 2004

Dynamic properties of a diluted pyrochlore cooperative paramagnet $(Tb_pY_{1-p})_2Ti_2O_7$

A. Keren[1,2], J. S. Gardner[3], G. Ehlers[4], A. Fukaya[5], E. Sagi[1], and Y. J. Uemura[5]
[1]*Department of Physics, Technion - Israel Institute of Technology, Haifa 32000, Israel.* [2]*Rutherford Appleton Laboratory, Chilton Didcot, Oxfordshire OX11 0QX, U.K.* [3]*Brookhaven National Laboratory, Upton, New York 11973-5000 and NIST Center for Neutron Research, National Institute of Standards and Technology, Gaithersburg, Maryland 20899-8562.* [4]*Institut Laue-Langevin, 6 rue J. Horowitz, 38042, BP 156-98042 Grenoble Cedex 9, France.* [5]*Physics Department, Columbia University, New York City, New York 10027, U.S.A.*
(Dated: March 22, 2022)

Investigations of the spin dynamics of the geometrically frustrated pyrochlore $(Tb_pY_{1-p})_2Ti_2O_7$, using muon spin relaxation and neutron spin echo, as a function of magnetic coverage p, have been carried out. Our major finding is that paramagnetic fluctuations prevail as $T \to 0$ for all values of p, and that they are sensitive to dilution, indicating a cooperative spin motion. However, the percolation threshold p_c is not a critical point for the fluctuations. We also find that the low temperatures spectral density has a $1/f$ behavior, and that dilution slows down the spin fluctuations.

The study of geometrically frustrated magnetic systems has introduced important new concepts to condensed matter physics including: order-by-disorder [1, 2], spin ice [3, 4, 5, 6], frustration driven distortion [7], and more. A recent and important addition is the concept of cooperative paramagnetism, whereby an interacting spin system dynamically fluctuates even as $T \to 0$ [8]. Cooperative paramagnetism on the pyrochlore lattice was first introduced in the study of $Tb_2Ti_2O_7$, where despite a substantial antiferromagnetic Curie-Weiss temperature of 20 K, a large Tb^{3+} moment of 9.4 μ_B fluctuates continuously down to $T = 50$ mK. Bulk and local probes have been used to study the magnetic nature and the lack of a phase transition in $Tb_2Ti_2O_7$[8, 9], and the results have been interpreted in terms of a cooperative spin system. However a unique experimental identification that the motion of one spin in $Tb_2Ti_2O_7$ influences the motion of its neighbors, is still lacking. Demonstrating conclusively that the fluctuations in $Tb_2Ti_2O_7$ are indeed a result of spin interactions, and testing to what extent the fluctuations are cooperative, is the main aim of this work.

Using muon spin relaxation (μSR) and neutron spin echo (NSE) we investigate the dynamic fluctuations on a wide time range in $(Tb_pY_{1-p})_2Ti_2O_7$ as a function of p. Here the non-magnetic Y ion replaces the magnetic Tb ion on the corner sharing tetrahedra which make up the pyrochlore lattice [10]. We vary p from 1, namely, a pure pyrochlore, to 0.21, which is below the percolation threshold $p_c = 0.39$ [11]. μSR and NSE allow us to determine the p dependence of the waveform and parameters for two important correlation functions (which are related). These are the auto correlation function $\langle \mathbf{S}_i(t)\mathbf{S}_i(0)\rangle$ where $\mathbf{S}_i$ is the spin operator on the i'th site, and the intermediate scattering function $\mathbf{S}(\mathbf{q},t)$ where $\mathbf{q}$ is the wavevector. If interactions are important, we expect the dynamic properties to be sensitive to p. Moreover, if an infinite number of spins participate in the fluctuations we expect a dramatic change of the correlation functions at p_c since at lower concentration the formation of an infinitely large island of spins is not possible. Our major finding is that, indeed, the spin fluctuations in $Tb_2Ti_2O_7$ result from interactions. However p_c is not a critical point, suggesting that spin groups of finite size fluctuate cooperatively. We also found that the time dependent part of the correlation function is a power law.

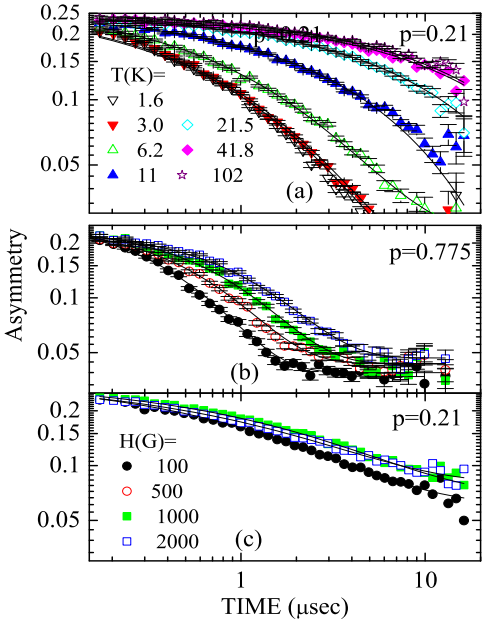


FIG. 1: (a) The muon asymmetry versus time at different temperatures for the most diluted sample. Between 102 and 42 K and below 3 K there is hardly any temperature dependence. (b) and (c) The muon asymmetry versus time at $T = 100$mK and various different fields for two samples. In (c) the error bars are omitted for clarity. The fits are to Eq. 1 as described in the text.

Our powder samples were made by the standard solid state method described elsewhere [8] and characterized by room temperature X-ray diffraction and temperature dependent magnetization. First we report on our μSR experiments, which were conducted at the ISIS pulsed muon facility, Rutherford Appleton Laboratory, UK. In these experiments we measure the time and field dependent asymmetry $A(H,t)$ of the decay positrons from muons implanted in the sample. This asymmetry is proportional to the muon polarization $P(H,t)$ along the $\widehat{\mathbf{z}}$ direction, which is the direction of the external field H. In Fig. 1 we present the asymmetry under three different conditions. The log-log plot is used to emphasize the difference in the asymmetries between different runs. In panel (a) we depict the muon asymmetry versus time at different temperatures for the most diluted sample. Note that between 102 and 42 K, and below 3 K, the muon polarization is almost temperature independent. In panel (b) and (c) we show the time dependence of the muon asymmetry at $T = 100$ mK for two different samples in various applied fields. At $p = 0.775$ the muon relaxation clearly decreases with increasing field. At a lower concentration $p = 0.21$ the relaxation is lower than that at $p = 0.775$ and again decreases between 100 and 1000G, but then saturates. In panel (c) the error bars are omitted for clarity. Temperature and field dependent raw data for the pure sample (which agree with ours) can be found in Ref. [8]. In all cases the raw data are fitted to a stretched exponential relaxation function

$$A(H,t) = A_0 \exp\left[-\left(t/T_1\right)^{\beta}\right] + B_g \qquad (1)$$

where B_g is a background signal representing muons that missed the sample, A_0 is the initial asymmetry, T_1 is the spin lattice relaxation time, and β is the stretching exponent. The fits were done with a common β for all temperature and fields for a given sample. The solid lines in Fig. 1 are from these fits. It is important to mention that T_1 obtained by such a fit is identical to that determined by the $1/e$ criteria ($A(H,T_1) = A(H,0)/e$).

The muon relaxation rate $1/T_1$ obtained from the fits at $H = 50$ G as a function of temperature for several samples is presented in Fig. 2. The observed temperature dependence of $1/T_1$ is very unusual. First of all $1/T_1$ shows no T dependence at the lowest T region for all p. This behavior is usually associated with paramagnetism, and it is observed in several frustrated magnets [12, 13, 14], low dimensional systems with singlet ground state and dangling bonds [15], and in high spin molecules [16]. Most magnets show a $1/T_1$ maximum at some critical temperature. Second, the slowing down of spin fluctuations occurs in two steps, one at high temperatures, followed by a plateau around 50 K, and another step starting around ~ 20 K. This might be a result of populations of a crystal field doublet which is 18 K above the ground state doublet [9]. Finally, both at very high and very low temperatures there are significant differences in $1/T_1$ between samples, however at 4 K, $1/T_1$ of

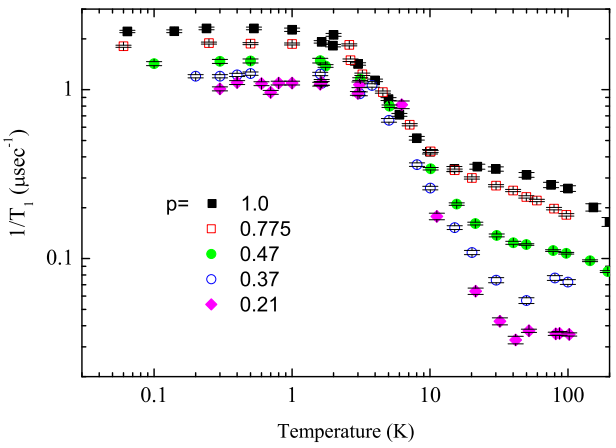


FIG. 2: Temperature dependence of the muon relaxation rate $1/T_1$ at H=50G.

all samples is the same. This is very intriguing and at present we have no explanation for this result. However, crystal field levels must be part of this explanation. In contrast, the p dependence of $1/T_1$ below 4 K is an indication that correlations are again playing a role in this low temperature region.

In Fig. 3 we present the muon relaxation time T_1 at $T = 100$ mK as a function of the longitudinal field for five samples. In all cases T_1 increases linearly as a function of fields at low fields. The solid lines are linear fits to the low field region. This region is not affected by diluting the pure system by 30%, but further dilution has a strong impact on $T_1(H)$. The dashed lines are continuations of the linear fits and serve as guides to the eye. The range in which $T_1(H)$ is linear decreases with decreasing p, and at low concentrations T_1 clearly saturates at $H \sim 0.5$ kG. More importantly, the more diluted the sample, the greater is the sensitivity of T_1 to H. This means that diluting the magnetic lattice slows down the spin fluctuation since the greatest sensitivity of T_1 to external field is when the spin system is static.

Analysis of the slope of $T_1(H)$ at low fields (dT_1/dH), and the exponent β from Eq. 1 as a function of p reveals more clearly the importance of interactions and percolation. In Fig. 4 we plot these parameters vs. p/p_c. The dotted lines are guides to the eye. Well above p_c the $\beta = 1$, namely, the muon relaxation is a pure exponential one, but as p decreases the nature of the muon relaxation changes gradually and becomes non-exponential with $\beta = 0.5$ well below p_c. Similarly dT_1/dH changes smoothly across the percolation threshold. Neither parameters depend critically on p_c. We therefore conclude that while the dynamical fluctuation are sensitive to interactions, they are not governed by percolating spins

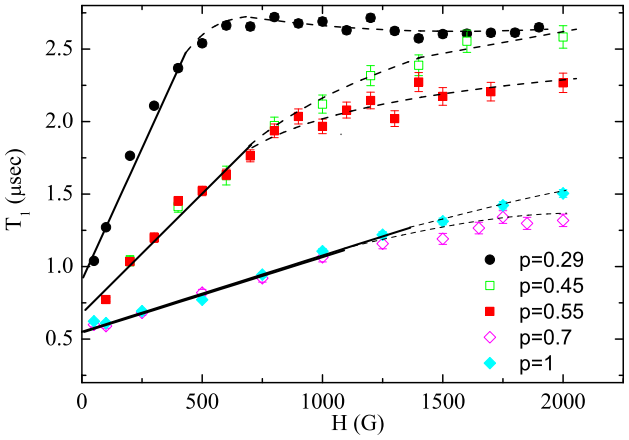


FIG. 3: The muon relaxation time T_1 as a function of the longitudinal field. The solid lines are linear fits of the low field region at $T = 100$ mK. dT_1/dH is obtained from the fits.

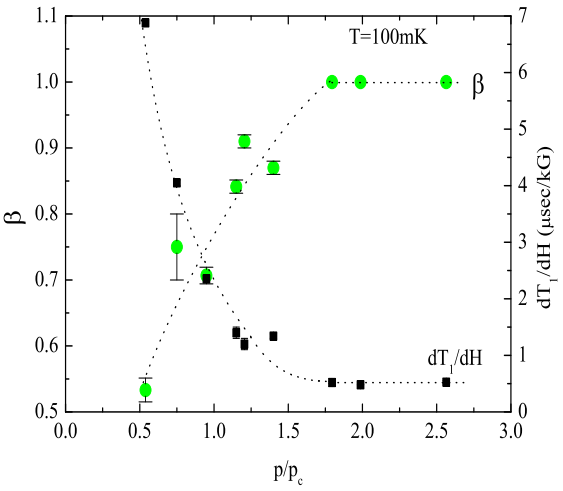


FIG. 4: dT_1/dH, and β vs. p/p_c where $p_c = 0.39$. The dotted lines are guides to the eye.

but rather by smaller groups of spins.

Next we present the NSE data on the same polycrystalline pure ($p = 1$) and diluted ($p = 0.37$) samples as in the μSR experiment. These experiments were performed at the Institut Laue-Langevin, France. The data from the pure sample only was briefly discussed in Ref. [17] and included here, with further analysis, for completion. In NSE experiments, which are reviewed in Ref. [18], a polarized neutron beam is used. The polarization is perpendicular to the magnetic field H, which is directed along the neutron's momentum. The neutron spins therefore precess, and the difference in the number of rotations in two identical magnetic fields before and after the sample is a direct measure of a velocity change (hence, the energy transfer) that the neutron suffered in the scattering process. By varying the field one controls the Fourier time $t = 1/^n\gamma H$, and the NSE method measures the scattering function $S(\mathbf{q}, t)$ in the time domain directly, in addition to the spatial domain ($\mathbf{q}$). The results are presented in Fig. 5 panels (a) and (b) after summing over several $\mathbf{q}$'s to reduces statistical error without affecting the $\mathbf{q}$ resolution significantly. This is possible since the magnetic signal is very broad in $\mathbf{q}$ [17] and NSE is a very poor $\mathbf{q}$ resolution technique. The relaxation is found to have two components: A fast one, which cannot be observed by the NSE experiment but leads to an immediate reduction of the normalized intermediate scattering function $S(\mathbf{q}, t)/S(\mathbf{q}, 0)$, and a slower one. In the pure sample (panel b) the relaxation of the slow component is consistent with a power law decay since it is linear on a log-log plot. In the diluted sample (panel a) no relaxation could be observed. The general evolution of the slow relaxing part of $S(\mathbf{q}, t)$ with doping is consistent with the μSR experiment. The more diluted the sample the slower the fluctuations are and the closer this fraction of the spins to static behavior. While this experiment does not elucidate on role of p_c it serves as a basis for a deeper understanding of the μSR data, especially the linear field dependence of the muon T_1, which is very unusual.

In all magnets with exponentially decaying correlation function, T_1 is a linear function of H^2 in the low field limit ($g\mu_B H \ll J$) relevant in the present case [19]. Using the NSE results we speculate on the origin of this linear field dependence and its evolution with doping. We consider only the slow relaxing part of the NSE data, since only this part is relevant in the μSR time window, and we make the assumption that

$$S(\mathbf{q}, t) = F(\mathbf{q})\Phi(t) \tag{2}$$

where $F(\mathbf{q})$ is not specified,

$$\Phi(t) = \frac{\tau_e^x}{(t + \tau_e)^x}, \tag{3}$$

x is the power of the correlation function, and τ_e is an early time cutoff introduced to normalize the correlation at $t = 0$. However, τ_e is so small that it can not be observed experimentally. It is therefore ignored in the denominator. Under this assumption the slope of the lines in Fig. 5 is x. The linear fit in panel (b) gives the x values shown in the figure. All these values are consistent with $x = 0.02$ with no q dependence. In the pure system, where the muon spin relaxation is exponential, T_1^{-1} is determined by the Fourier transform of the auto correlation function $\langle \mathbf{S}_i(t)\mathbf{S}_i(0)\rangle$ at the frequency $f = \frac{\gamma_\mu}{2\pi}H$ [19]. This correlation function is related to the sum over $\mathbf{q}$ of $S(\mathbf{q}, t)$ [20]. Therefore, under the assumption of Eq. 2 we

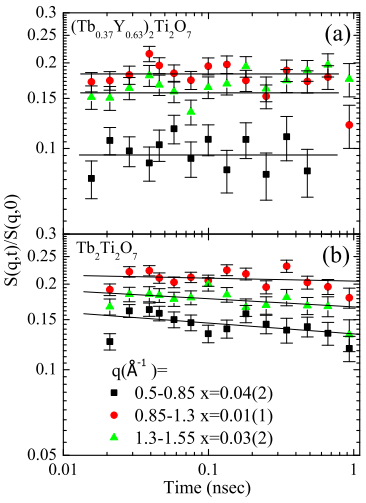


FIG. 5: Neutron Spin Echo measurements in two $(Tb_pY_{1-p})_2Ti_2O_7$ samples presented on a log-log scale. The solid lines are linear fits (x is the slope).

have

$$\frac{1}{T_1(H)} = 2\Delta^2 \int_0^\infty \Phi(t)\cos(\gamma_\mu H\tau)d\tau. \qquad (4)$$

where $2\Delta^2 = \gamma_\mu^2 \langle \mathbf{B}_\perp{}^2 \rangle$ is the RMS of the instantaneous transverse (to H) field distribution at the muon site (from the slowly fluctuating part only). This gives

$$\frac{1}{T_1} = \frac{2\Delta^2(2\pi f\tau_e)^x}{2\pi f}\Gamma(1-x)\sin\left(\frac{\pi x}{2}\right). \qquad (5)$$

In our experiment $x \to 0$, therefore [21]

$$T_1(H) \simeq \frac{2f}{x\Delta^2}. \qquad (6)$$

Thus, on the basis of Eqs. 2 and 3 we can explain the linear field dependence of the muon T_1. We associate the fact that $T_1 > 0$ even when $H = 0$ with the presence of static fields from other sources such nuclear moments for example.

To increase confidence in Eq. 6 we check if reasonable values for the theoretical parameters produce the observed T_1. For example if $\tau_e \sim 10^{-13}$ sec, $\mathbf{B}_\perp$ and H on the order of 100 G ($2\pi f \sim \Delta \sim 10$ MHz) and $x = 0.02$, we have $(2\pi f\tau_e)^x \sim 1$ and $T_1 \sim 1\ \mu$sec, on the order of the measured value. We thus believe that Eq. 6 describes our μSR results appropriately.

This allows us to conclude further that steeper $T_1(H)$ implies smaller $x\Delta^2$. We argue that it is mostly x that is changing with decreasing p and not Δ. First, as observed in the NSE experiment, x decreases with decreasing p. Second, the drastic change in dT_1/dH near p_c cannot be due to a dramatic change in Δ. This parameter, which measures the local field at the muon site, certainly depends on p, but it is not sensitive to whether there is, or is not, percolation in the system. Therefore, the slowing down of spin fluctuations with decreasing p is manifested by a decreasing x, namely, the power law decay becomes closer to a constant.

To summarize, our measurements clearly classify the pyrochlore $(Tb_pY_{1-p})_2Ti_2O_7$ as a cooperative paramagnet. The name "paramagnet" is justified by the plateau in $1/T_1$ at low temperature. The adjective "cooperative" is appropriate since the spin dynamics depend on the coupling between magnetic moments. However, whether the spin system percolate or not is not relevant. For comparison in the kagomé based compound $SrCr_{9p}Ga_{12-9p}O_{19}$ spin dynamic was shown to be completely impartial to p_c [13]. We also show that the correlation of spins in this magnet has a power law decay with a very small power x. This power gets even smaller when the magnetic coverage decreases resulting in slowing down the spin fluctuations. Since the Fourier transform of t^{-x} behaves asymptotically like f^{x-1} the fluctuation spectrum practically has $1/f$ behavior in the frequency range 0.5 MHz to 50 GHz.

We would like to thank the ISIS facilities for their kind hospitality and continuing support of this project. This work was funded by the Israel - U. S. Binational Science Foundation, the EU-TMR program, and the NATO Collaborative Linkage Grant, reference number PST.CLG.978705. JSG's work at Brookhaven is supported by Division of Material Sciences, U.S. Department of Energy under contract DE-AC02-98CH10886.

[1] S. T. Bramwell, M. Gingras and J. N. Reimers, J. App. Phys. **75,** 5523 (1994).
[2] J. D. M. Champion et al. Phys. Rev. B **R68**, 020401 (2003).
[3] P. W. Anderson, Phys. Rev. **102**, 1008 (1956).
[4] M. J. Harris *et al.*, Phys. Rev. Lett. **79**, 2554 (1997).
[5] A. P. Ramirez *et al.,* Nature **399**, 333 (1999).
[6] S. T. Bramwell and M. J. P. Gingras, Science **294**, 1495 (2001).
[7] K. Terao, J. Phys. Soc. Jpn, 1413 (1996); Y. Yamashita and K. Ueda, Phys. Rev. Lett. **85**, 4960 (2000); A. Keren and J. S. Gardner, Phys. Rev. Lett. **87**, 177201-1 (2001); Oleg Tchernyshyov, R. Moessner, and S. L. Sondhi, Phys. Rev. Lett. 88, 067203 (2002); P. Carretta *et al.,* cond-mat/0205092.
[8] J. S. Gardner *et al.*, Phys. Rev. Lett. **82**, 1012 (1999).
[9] M. J. P. Gingras *et al.*, Phys. Rev. B **62**, 6496 (2000).
[10] Subramanian *et al.,* Prog. Sol. State Chem. **15**, 55 (1983).

[11] C. L. Henley, Can. J. Phys. **79**, 1307 (2001).
[12] Y. J. Uemura *et al.*, Phys. Rev. Lett. **73**, 3306 (1994).
[13] A. Keren *et al.*, Phys. Rev. Lett. **84**, 3450 (2000).
[14] J. Hodges *et al.*, Phys. Rev. Lett. **88** 077204 (2002).
[15] K. Kojima *et al.*, Phys. Rev. Lett. **74**, 2812 (1995); K. Kojima *et al.*, Phys. Rev. Lett. **74**, 3471 (1995).
[16] Z. Salman *et al.*, Phys. Rev. B. **65**, 132403 (2002).
[17] J. Gardner *et al.,* Phys. Rev. B **68**,180401R (2003).
[18] F. Mezei, C. Pappas, Th. Gutberlet (eds.) Lecture Notes in Physics Vol. **601**, Springer, Berlin, Heidelberg (2003).
[19] A. Keren *et al.*, Phys. Rev. B. **64**, 054403 (2001).
[20] A. Keren *et al.*, Hyp. Int. **85**, 363 (1994).
[21] We use $\Gamma(1-x)\sin(x\pi/2) = x\pi/2 + O(x^2)$.